Original Article
A systems biology approach to study the phagosomal proteome modulated by mycobacterial infections

Prahlad K. Rao[1], Christoher R. Singh[2], Chinnaswamy Jagannath[2], and Qingbo Li[1,3]

[1]Center for Pharmaceutical Biotechnology, University of Illinois at Chicago, Chicago, IL 60607, USA; [2]Department of Pathology and Laboratory Medicine, University of Texas Health Sciences Center, Houston, TX 77030, USA; [3]Department of Microbiology and Immunology, University of Illinois at Chicago, Chicago, IL 60612, USA.

Abstract: Systems biology and proteomics have recently contributed significantly to the insight into the biogenesis and immunity-related functions of the phagosome. To gain insight into the modulation of the phagosomal proteome by the wild-type *Mycobacterium tuberculosis* H37Rv reference strain, an attenuated mutant of the H37Rv strain, and the BCG Pasteur vaccine strain, we employed the nano-liquid chromatography/LTQ-FTMS based proteomics approach and a systems biology approach to analyze the bacillus-containing phagosomes purified from the bone-marrow-derived BMA3.A3 macrophages infected with the three different mycobacterial strains. We identified 322 proteins at a false-discovery rate of 2%. These proteins were quantified with a label-free proteomics method. All but one of these proteins is mouse proteins. The gene ontology analysis of these mouse proteins suggests that lysosomal proteins represented <3% of the detected proteins, supporting the observation that these mycobacterial strains inhibit or limit the phagosome maturation process. The results also indicate that the endoplasmic reticulum (ER) proteins do not constitute a major part of the phagosome proteome, supporting the phagosome maturation model of the role of ER in phagosome biogenesis. This phagosome maturation model is in contrast to the phagocytosis model which predicts that half of the phagosome membrane is derived from ER. This pilot study demonstrates that a combination of proteomics, multivariate analysis, and systems biology promises to bring forward new insights into the mycobacterial pathogenesis and the interconnected phagosome biology.

Key words: Phagosome, systems biology, mycobacterium tuberculosis, proteomics, macrophage

Introduction

Macrophages use phagocytosis to control pathogens. While the maturation of phago-somes into phagolysosomes is critical to destruct invading infectious agents, the exceptional success of *Mycobacterium tuberculosis* (Mtb) as an intracellular pathogen depends largely on its remarkable ability to modulate the exact process of phagosome maturation to avoid being killed in a phagolysosome [1, 2]. Phagosomes are specialized membrane-bound organelles. They are generated in phagocytic cells such as macrophages. They engulf micro-organisms, uptake foreign particles, internalize apoptotic cells, mount an immune response, or maintain tissue homeostasis [3]. A nascent phagosome undergoes a complex maturation process involving sequential fusion with early endosomes, late endosomes, and lysosomes [4]. Once it matures, the phago-lysosome degrades the engulfed material to facilitate antigen presentation in a highly controlled manner [5-7].

Proteomics has recently contributed signify-cantly to the insight into the biogenesis [8, 9] and immunity-related functions of the phago-some [10, 11]. The proteome profiles of latex bead-containing phagosomes have been studied in cell lines from mice [8, 10, 12, 13], *Drosophila sp.* [6], *Dictyostelium discoideum* [14], and *Entamoeba histolytica* [15]. These studies improve our understanding of phago-some maturation and modulation by cytokines. Valuable insights into subcellular vacuoles containing pathogenic microorganisms were also obtained by infection of mammalian

phagocytes with *Francisella tularensis* [16], *Mycobacterium avium* [17], *Salmonella typhimurium* [18], *Yersinia pseudotuberculosis* [18], *Listeria innocua* [19], *Rhodococcus equi* [20], *Leishmania* parasites [21], and *Legionella pneumophila* [22, 23].

In contrast, there has been a limited proteomic study of the mycobacterial phagosome in the literature [24]. In this pilot study, we explored the nano-liquid chromatography/mass spectrometry-based proteomic approach [25] in combination with a systems biology analysis [6] to study the mycobacterial phagosomes from BMA.A3 macrophages infected with three different mycobacterial strains. The results provide an insight into the regulation of proteome composition and interaction network in the phagosomes infected with different mycobacterial strains. The demonstrated methodological platform will likely be useful for simultaneous analysis and comparison of the modulation of phagosomal proteomes by different pathogen strains at different infection conditions.

Materials and methods

Purification of mycobacterial phagosome samples

The BMA.A3 macrophage like cell line was derived from bone marrow derived macrophages of C57Bl/6 mice and was a kind gift of Dr. Kenneth L. Rock (U. Massachusetts, USA). We harvested bacillus-containing phagosomes from macrophages infected by the wild type reference Mtb H37Rv lab strain (ATCC27294), the ΔfbpA mutant strain derived from Mtb H37Rv [26], and the BCG Pasteur vaccine strain. The three mycobacterial strains were respectively used to infect BMA.A3 macrophages derived from the C57Bl/6 mouse bone marrow as described and the phagosomes were purified by the method described earlier [27]. Specifically, the macrophages were infected with the mycobacteria (MOI 1:5) for 4 hrs with gentle mixing, washed thrice with McCoys medium and incubated for another 18 hrs. The macrophages were scraped, washed thrice in a phagosome fractionation buffer (PFB) with 10 mM Hepes, 5 mM EDTA, 5 mM EGTA, pH 7.0 and suspended in PFB with an anti-protease mix consisting of 1 µg/mL leupeptin, 1 µg/mL pepstatin and 1 mM phenylmethyl sulfonylfluoride. Pellets were then homogenized in a glass tissue homo-genizer 10 times and passed 10 times through a 28-gauge needle. Lysates were centrifuged at 500 *g* for 5 min to sediment nuclei and the post nuclear supernatant was layered on a step gradient of 50% and 12% sucrose in the PFB. After centrifugation at 1000 *g* for 60 min, the interphase of phagosome fraction was collected and further purified by passing through two successive cushions of 70 kDa and 400 kDa ficoll in the PFB. The final purified phagosomal pellet was collected by centrifugation at 10,000 *g* for 15 min, suspended in an SDS/PAGE sample buffer, heat-killed, further lysed with bead-beating [28], and fractionated with SDS/PAGE electrophoresis for proteomics analysis as described below.

Proteomic analysis of bacillus-containing phagosomes

Briefly, *ca.* 100 µg of proteins from each bacillus-containing phagosome sample was fractionated into five SDS/PAGE gel fractions as described [29]. The peptide extract from each fraction was purified with a ZipTip [28] before analysis with a nanoLC/LTQ-FTMS system at the Proteomics and Informatics Facilities Services in the Research Resources Center at University of Illinois at Chicago (PISF-RRC-UIC) which is supported by the Searle Funds at the Chicago Community Trust. In this experiment, each peptide extract sample was injected once. A total of 15 LC/MS injections were performed for the three phagosome samples. With the Sorcerer server (Sage-N Research, Inc.; Milpitas, CA) hosted at the PISF-RRC-UIC, we searched the RAW data files against a composite database containing the protein databases of mouse, H37Rv, BCG, and their reversed decoy databases. We used the decoy databases to control FDRs in peptide and protein identifications [30, 31]. Specifically, the RAW data files were converted to mzXML files with the Trans-Proteomic Pipeline software [32]. The mzXML files were searched against the composite database. The peptide mass tolerance was set at 15 ppm with methionine oxidation as a differential modification. We allowed up to 2 missed cleavages and an isotope check using a mass shift of 1.003 amu. We only accepted MS/MS identifications with peptide probability above 0.5 for quantitation.

Results

Protein identification and quantitation

From the three phagosome samples, we identified a total of 6428 peptide charge states (PCSs) [33] at an FDR of 5%. After an analysis with the Trans-Proteomic Pipeline software [32], redundant PCSs were removed to result in 3086 unique PCSs. We quantified the abundance of each PCS with the label-free method as described previously [28-30]. With the procedure to align chromatograms and cross-reference PCSs, a PCS identified in one sample can also be quantified in the other two. This procedure increases the number of proteins that can be quantified [29]. A PCS abundance is expressed as an XIC intensity. An XIC intensity is the integration of a peptide mass spectrometric ion current intensity over a specified liquid-chromatography (LC) elution-time window. This LC elution-time window corresponds to the LC peak width of the PCS [28]. Because each sample was fractionated into five SDS/PAGE gel bands, the PCS XIC intensities were median-normalized in each SDS/PAGE gel fraction respectively. The 3086 unique PCSs were then combined and assembled into 472 unique proteins by an approach similar to that described previously [29, 34]. Among the 472 proteins, 327 had ≥2 unique PCSs. Five of these 327 proteins were the hits from the decoy databases and were removed as false positives. Thus, we identified 322 unique proteins at an FDR of 2% (data available from the Author upon request). All but one of these 322 proteins is from the mouse proteome. The abundance of a protein was calculated by summing the PCS XIC intensities for that protein [28, 30]. Finally, the protein XIC intensities in each sample were normalized by the summed XIC intensities for that sample. The XIC intensities correlates positively with protein abundance although they do not necessarily represent the accurate absolute amount of a protein [28]. Because the same set of PCSs were used to calculate the XIC intensity of a protein in all of the three samples, the XIC intensities of the protein can be directly compared to assess its relative abundance in the three samples [28]. The XIC intensities are adequate to compare the difference in expression abundance among the three samples because they have been normalized to the summed XIC intensities in each sample respectively. In this study, we do not intend to use the XIC intensity to represent the absolute protein abundance because that will require a calibration process with internal

standards [28, 35]. At a qualitative scale, however, a higher XIC intensity usually indicates that a protein is expressed at a higher abundance.

Principal component analysis

Because we have three phagosome samples in this study, a pair-wise analysis will require comparing three sample pairs separately. To facilitate a convenient overview of the protein expression profiles and to visualize the differences among them in a concise way, we performed a principal component analysis (PCA) on the 322 x 3 matrix that contains the XIC intensities of the 322 proteins in the three different phagosome samples (data available from the Author upon request). PCA is a statistical analysis technique utilized in many fields including proteomics research [36]. It is an intuitive method that reduces a larger number of variables to a smaller number of groups that can be more readily visualized and understood [37]. The PCA was performed as previously described [30]. The analysis resulted in two principal components, PC1 and PC2, which explained 58% and 42% variances respectively. The PCA reduces the original three-dimensional data space i.e., XIC intensities from the three samples into the two-dimensional space defined by PC1 and PC2. The resulted graph is easier to visualize and compare as shown in a biplot in **Figure 1**. The three vectors represent the three different samples. They are noted as Φ_{BCG}, $\Phi_{\Delta fbpA}$, and Φ_{H37Rv} respectively where Φ represents a phagosome and a subscript indicates the mycobacterial strain that it contains.

In **Figure 1**, the proteins with minimal differences among the three samples tend to cluster around the origin of the space defined by the PC1 and PC2 axes. Proteins with increasing difference among the three samples distribute further away from the origin. When a protein has a significantly higher XIC intensity in one sample than in the other two, it reaches far out along the vector of that sample. Examples are the proteins Mrps28 and Nup210 for $\Phi_{\Delta fbpA}$, proteins Ptcd3 and Rpi26 for Φ_{BCG}, and proteins C230096C10Rik and Rab11b for Φ_{H37Rv} (**Figure 1**).

The multivariate distance of a protein from the dataset center i.e., the origin of the space defined by PC1 and PC2 is quantitatively
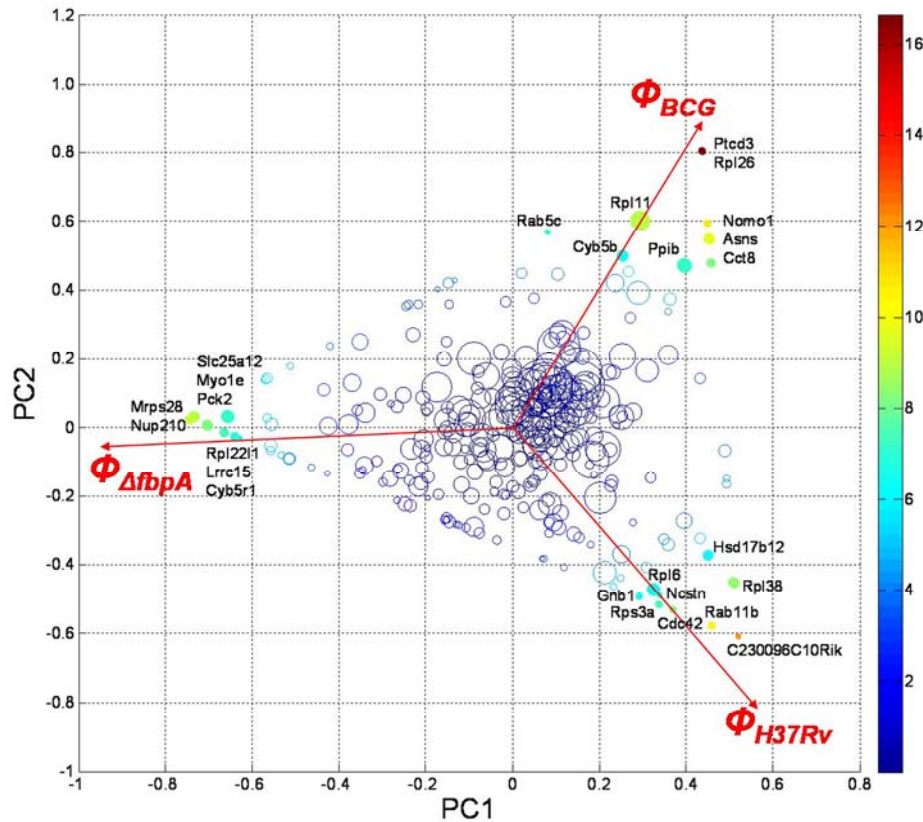
Figure 1. Scatter plot of the T2 values and the PCA scores on PC1 and PC2 of the 322 proteins quantified in the phagosomes (*Φ*) of the BCG-, ΔfbpA-, and H37Rv-infected macrophages respectively. To the right is the color map of the T2 values which has a median of 0.88. Each colored marker represents a protein. The marker size is proportional to the square-root of the averaged XIC intensity of that protein in the three phagosome samples.

measured by the Hotelling's T2 value [30]. The T2 value represents the index of gross change of a protein among the three samples. To determine the statistically significant proteins that are associated with each sample, we calculate a critical value by:

$$T_C^2 = \frac{(n-1)p}{(n-p)} F_{\alpha;p,n-p}$$

where *n* is the number of proteins, *p* is the number of principal components, *α* is the confidence interval, and *F* is the F-statistic with (*p*, *n* – *p*) degrees of freedom. A protein with a T2 value > T_C^2 is considered statistically significant at the level of *α*. Here, we use *α* = 0.05 which results in T_C^2 = 6.07. In **Figure 1**, the proteins with T2 > 6.07 are represented by

the filled makers. The names of these proteins are labeled in **Figure 1**.

In **Figure 1**, the average XIC intensity of each protein is indicated by the size of its marker. Basically, the diameter of each circular marker is proportional to the square-root of the average XIC intensity of a protein in the three samples. An XIC intensity qualitatively correlates with the absolute abundance of a protein when different proteins are compared. It can be seen that a majority of the proteins, especially the abundant ones, have similar abundances in the three phagosome samples, have low T2 values, and thus cluster around the center of the dataset. The PCA also reveals that each sample has some proteins closely related to it as shown by the close vicinity of those proteins to the vector representing that sample (**Figure 1**). The three vectors
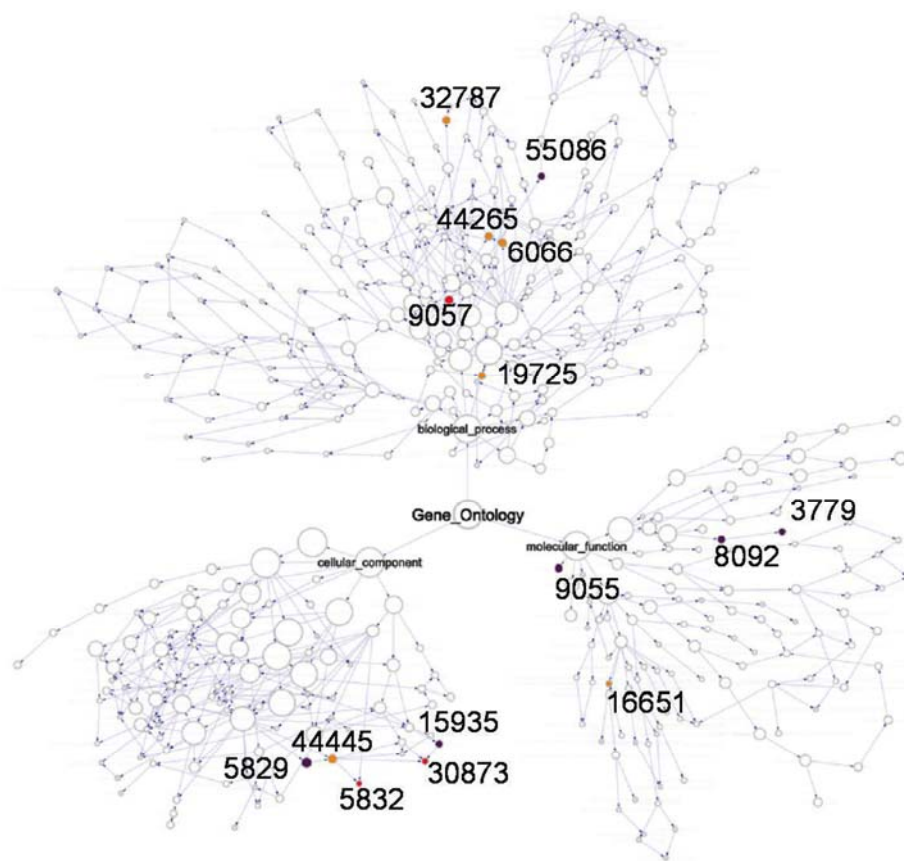
Figure 2. A full GO analysis of the 321 mouse proteins detected in the mycobacterial phagosomes. The colored nodes represent the GO terms with ≥5 proteins and have a >3-fold change in ≥1 one sample pair. The red, purple, and orange node colors indicate that a GO has: (red) a >3-fold change in ≥2 sample pairs; (purple) a >3-fold change in one sample pair and a 2- to 3-fold change in another sample pair; (orange) a >3-fold change in one sample pair. The GO IDs are labeled for these regulated nodes. The white nodes represent the GO terms that are not regulated (≤3-fold) and those that are not enriched (*p* ≥.05) but are parents of an enriched GO term.

representing the three samples distribute approximately to the three corners of a triangular. Thus, the proteomic results suggest a differential modulation of the phagosomal proteome by the three different mycobacterial infections. The PCA intuitively summarizes the differentially expressed proteins to simplify the comparison of protein expression difference among the three samples (**Figure 1**). There are 26 proteins which T2 values are higher than the critical threshold of 6.07. Each of these 26 proteins has an XIC intensity in one sample ≥70% of the combined XIC intensity from the three samples. Except for Rab5C, all other 25 proteins have a maximum XIC intensity among the three samples ≥3-fold higher than either of the rest of two. We notice, however, that some

proteins having a ≥3-fold change between two samples are not identified as a significant difference if the proteins are not the most abundance ones among the three samples. Thus, the T_C^2 = 6.07 cutoff results in a conservative assessment of the significance of a change in protein abundance among the three samples. Although the PCA intuitively identifies the proteins that are closely related to each of the three sample, the significance of the relative abundance of individual proteins still requires additional statistical analysis with adequate replicates [29]. Replicate analyses were not addressed in this pilot study. Thus, we refrain from further interpreting individual proteins.
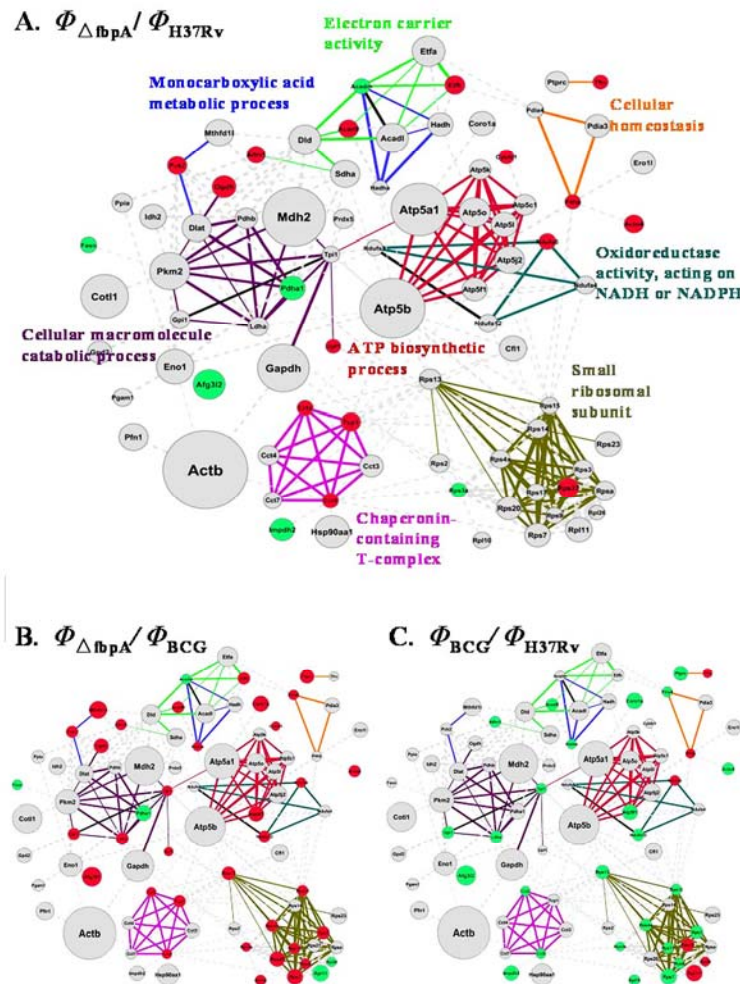
Figure 3. Interaction network of the 81 proteins from the regulated GO terms. The network is overlaid with protein differential expression data for sample pair $\Phi_{\Delta fbpA}/\Phi_{H37Rv}$ (panel A), $\Phi_{\Delta fbpA}/\Phi_{BCG}$ (panel B), or Φ_{BCG}/Φ_{H37Rv} (panel C). Protein clusters/modules are annotated in panel A with text labels. The sizes of the nodes are proportional to the average XIC intensities of the proteins in the three phagosome samples. The thickness of an edge is proportional to the confidence score of the interaction. The red, gray, and green node colors indicate that a protein is upregulated (>3-fold), unchanged, or downregulated (<0.33-fold). Different edge colors are used to distinguish the eight different protein clusters as indicated with the color-matching text labels in panel A. The gray dashed edges indicate that the interactions are not within one of the eight clusters. The black edges are the ones shared by ≥2 protein clusters. The node labels represent the protein names annotated with BioMart (www.Biomart.org).

In the following, we use a systems biology approach [6, 25] to find the protein sets that are enriched in the bacillus-containing phagosomes. We then examine the differential regulation of the proteins in those enriched proteins sets.

Regulated GO terms

For the 321 mouse proteins, we identify 341 enriched GO terms (p <.05) in the full GO annotation that includes *biological_process, cellular_component, and molecular_function* [38] by using the BiNGO plug-in in Cytoscape [39]. We further determine the enriched GO terms that are regulated in the three sample pairs i.e., $\Phi_{BCG}/\Phi_{\Delta fbpA}$, Φ_{BCG}/Φ_{H37Rv}, and $\Phi_{\Delta fbpA}/\Phi_{H37Rv}$ where Φ represents phagosome and a subscript indicates the mycobacterial strain that infected the macrophage. To

determine whether a GO term is regulated in a sample pair, we perform a t-test [29] for a GO term with ≥5 proteins by using the log2-transformed protein XIC intensities. We combine the results from the three sample pairs and select 15 GO terms that are regulated with >3-fold change (p <.05) in at least one sample pair. These 15 regulated GO terms are indicated with colored nodes in the GO network (**Figure 2**). Their annotations and the proteins in each GO term are available from the Author upon request. There are 104 unique proteins in these 15 regulated GO terms. The GO network analysis provides an overview of the themes of biological process, molecular function, and cellular component in the phagosomes modulated by the three different mycobacterial infections. To further examine the regulation of the proteins contained within these GO terms, we construct a protein interaction network in the following.

Interaction networks among the proteins in the regulated GO terms

We examine the protein network underlying the affected biological themes i.e., GO terms. For this purpose, we perform a network analysis for the 104 proteins from the 15 regulated GO terms with String [40, 41]. Medium-confidence interactions are extracted for 81 of the 104 proteins from the String database [41]. **Figure 3** shows the interaction network of these 81 proteins. These 81 proteins can be divided into approximately eight modules. The edges representing the interactions within one of these eight modules are colored differently to distinguish them from those in other modules (**Figure 3A**). These eight modules include (a) chaperonin-containing T-complex, (b) oxidoreductase activity, acting on NADH or NADPH, (c) cellular homeostasis, (d) monocarboxylic acid metabolic process, (e) cellular macromolecule catabolic process, (f) electron carrier activity, (g) ATP biosynthetic process, and (h) small ribosomal subunit. The descriptions of these eight protein clusters are indicated with the colored text labels in **Figure 3A**. Many high-abundance proteins in the network are not regulated, as expected. A t-test (p<.05) and a 3-fold change threshold were used to assess the regulation of these eight modules in the three sample pairs i.e., $\Phi_{BCG}/\Phi_{\Delta fbpA}$, Φ_{BCG}/Φ_{H37Rv}, and $\Phi_{\Delta fbpA}/\Phi_{H37Rv}$. Only the chaperonin-containing T-complex was found to be regulated in $\Phi_{BCG}/\Phi_{\Delta fbpA}$, and $\Phi_{\Delta fbpA}/\Phi_{H37Rv}$

with statistical significance.

While the GO analysis described previously (**Figure 2**) provides a higher level overview of the biological effects of a mycobacterial infection on the phagosome, the protein interaction network described in **Figure 3** reveals the gene products and their interactions that might affect those changes. The protein clusters identified through this process will be useful to more confidently assess the modulation of the phagosome by mycobacterial infections. This approach is also biologically relevant because many enzymes involve multiple subunits to function. In addition, an enzyme that catalyzes a biochemical reaction most likely interacts with other proteins in the same pathway [42].

The protein network analysis is probably useful to decipher the roles of those proteins that participate in multiple pathways. Those proteins are difficult to evaluate for their roles based on the conventional one-gene-one-phenotype model because of a potential pathway cross-talk. The modular analysis shown in **Figure 3** will be useful to reveal the pathway crosstalk and to determine the function of a protein. For example, the electron carrier activity module and the monocarboxylic acid metabolic process module intertwine and share Acadl and Acadm. Thus, the regulation and the role of Acadl and Acadm should be considered together with the regulation of proteins in both the electron carrier activity module and the monocarboxylic acid metabolic process module. The preliminary results obtained here suggest that the sample pair $\Phi_{\Delta fbpA}/\Phi_{H37Rv}$ bears more similarity than $\Phi_{\Delta fbpA}/\Phi_{BCG}$ or Φ_{BCG}/Φ_{H37Rv}. This was expected since $\Delta fbpA$ is a mutant derived from Mtb wild type H37Rv while BCG was derived from *M. bovis* a species related to Mtb. Further statistical analyses of the differential expression for these eight modules with a *t*-test (p<.05) and a 3-fold change cutoff, however, found that only the chaperonin-containing T-complex to be statistically significant in differential expression among the three samples. There are two possible reasons. First, for many proteins, the abundance difference among the three samples is relatively small (**Figure 1**). Second, the variation of differential abundance ratios is relatively large in the modules. More replicates will be needed to increase the statistical power to discern the more subtle difference among

Figure 4. The *cellular_component* GO hierarchy of the 321 detected mouse proteins. The GO hierarchy contains 304 of these 321 proteins. The colored nodes represent the overrepresented GO terms (*p*<.05). The yellow to orange colors indicate an increase in the confidence of the overrepresented GO term. The white nodes represent the GO terms that are not overrepresented but are parents of an enriched GO term. The lower-lever GO terms can be divided into 10 clusters corresponding to different organelles, complexes, or compartments. The numbers of proteins in these clusters and several higher-level GO terms are indicated in the parenthesis. The solid edges indicate the main hierarchy of the GO terms. The 10 GO clusters are given names corresponding to the organelle, complex, or compartment they belong, and are indexed with Roman numbers. Each GO cluster is enclosed with a red dashed-line envelope. The names of some selected GO terms are labeled in each GO cluster.

these phagosomes modulated by the three different mycobacterial strains. Nevertheless, the graph in **Figure 3** is useful to provide an overview of the changes in relative abundance of the proteins in the regulated GO terms shown in **Figure 2**.

Organellar and compartmental distribution of the proteins

To obtain a distribution profile of the detected mouse proteins in organelles and compartments, the *cellular_component* branch of the full GO hierarchy in **Figure 2** is examined in greater details as shown in **Figure 4**. Of the 321 mouse proteins, 304 are annotated in the GO term of *cellular_component*. There are 256 proteins assigned to *organelle*. The over-represented GO terms of *membrane-bound organelle* and *intracellular non-membrane-*

bound organelle have 196 and 87 proteins respectively. To track the important GO terms that effect the over-representation of the GO hierarchy in **Figure 4**, we track down the GO terms at the end of the GO hierarchy tree. These lower-level GO terms, as represented by relatively smaller nodes, can be divided into 10 major clusters based on the organelle, compartment, or complex that they belong to. Of these 10 clusters of GO terms, mitochondrion (II) has the largest number of proteins to represent 36% of the proteins in the *cellular_component* GO hierarchy (**Figure 4**). Here, a Roman number in parenthesis indicates the GO term cluster identified in **Figure 4**. The combined number of unique proteins in microsome (I) and endoplasmic reticulum (ER) (II) is 35, representing 12% of the proteins in *cellular_component*. Of the 11 proteins in microsome (I), only three are

unique compared to those in ER (III). This is not surprising because microsome originates from ER. There are nine proteins belong to cytoplasmic membrane-bounded vesicle (IV) which represents 3% of the proteins in the *cellular_component* GO hierarchy. There are also only nine proteins from lysosome (V). This is consistent with the known observation that mycobacterial phagosomes do not fuse with lysosomes. The eight proteins in ATPase (VI) actually are mitochondrial proteins although they are identified as a separate cluster that is related to protein complex due to network interdependence. There are 32 proteins belonging to cytoskeleton (VII). Six proteins are identified for the chaperonin-containing T-complex (VIII). There are 42 identified ribosomal proteins (IX) which represents the second largest group of proteins identified from the samples. Twelve proteins (4%) are from chromatin (X), probably due to some degree of contamination from the nucleus. Nine of these 12 proteins belong to nucleosome.

Intraphagosomal mycobacterial proteins

Of the 322 proteins detected at an FDR of 2% from the mycobacterial phagosomes, only one belongs to the mycobacteria. It is the probable iron-regulated elongation factor Tu (EF-Tu; Rv0685; BCG_0734). This protein was identified from culture supernatants [43], from cell wall [44], and upregulated inside macrophages [45] or under a high-iron condition [46]. In this study, the EF-Tu differential expression ratio in the three sample pairs i.e., $\Phi_{\Delta fbpA}/\Phi_{H37Rv}$, $\Phi_{\Delta fbpA}/\Phi_{BCG}$, and Φ_{BCG}/Φ_{H37Rv}, was 4-, 1-, and 5-fold respectively. It appears that the BCG vaccine strain and the candidate vaccine strain ΔfbpA have similar EF-Tu expression in the phagosomes, while H37Rv has the EF-Tu abundance several folds lower in the phagosomes. The lower abundance of EF-Tu in the H37Rv-containing phagosomes could be due to reduced expression or increased secretion which a further protein dynamic analysis will confirm [28]. It is an essential gene for *in vitro* growth of H37Rv shown by the Himar1-based transposon mutagenesis [47]. However, its essentiality for *in vivo* Mtb survival remains to be elucidated.

At an FDR of 28%, 30 mycobacterial proteins were identified in a list of 923 proteins identified from the three mycobacterial phagosome samples. This high FDR and the small number of the mycobacterial proteins do not allow us to perform a protein network analysis for the intracellular mycobacteria. A more in-depth analysis of the mycobacterial phagosomes in the future will be necessary to obtain confident results to assess the intraphagosomal mycobacterial metabolic pathways and host-pathogen interaction networks.

Discussion

To study the phagosomal proteome modulated by intracellular antigenic mycobacteria, we have utilized a proteomics approach in combination with a systems biology analysis to compare the effect of mycobacterial infections on the phagosomal proteome. We used three mycobacterial strains to infect the BMA.A3 macrophages respectively, including H37Rv, BCG, and the ΔfbpA mutant strain derived from H37Rv [27]. BCG, an attenuated strain of *M. bovis*, is highly similar to Mtb in antigenic composition. Both BCG and H37Rv inhibit the fusion between lysosomes and phagosomes thus arrest the maturation of the phagosomes. The ΔfbpA strain, however, showed an enhanced capacity to fuse with late endosomes to allow limited maturation of the phagosomes. Thus, ΔfbpA is more immunogenic in macrophages due to its enhanced susceptibility to oxidants in macrophages and increased maturation. The percentages of phagosomes positive for several markers of late-endosomes and lysosomes e.g., LAMP-1, Hck, and CD63 were found to be *ca*. 2-fold higher in the phagosomes from the ΔfbpA-infected macrophages than in those from either the BCG- or H37Rv-infected macrophages based on fluorescence microscopic image analysis [27]. In this study, LAMP-1 was detected with <3-fold change among the three samples (**Figure 3**). Within the 3-fold cutoff threshold, the protein expression level for LAMP-1 is not considered to be differentially expressed among the three samples. Another lysosome marker, Rab7, was also not regulated in this proteomic study, consistent with the result that the Rab7 level was approximately identical in the three phagosome samples based on the fluorescence microscopic image analysis in the previous study [27]. In that previous study, we had demonstrated that the mycobacterial phagosomes including those from virulent wild type H37Rv acquire the early endosome marker rab5 as early as 4 hrs but do not acquire rab7, a lysosomal marker even after 24 hrs after phagocytosis. Thus, we chose to analyze the

wild type H37Rv as a reference strain and compared this with our novel ΔfbpA mutant that was shown to progress in maturation to late endosomal stage and acquire CD63 but not rab7. BCG had an intermediate phenotype of rab5 positivity and excluded rab7 as well as CD63. From our previous studies, it was apparent that BCG and H37Rv would be in a rab5 'arrested early endosome' stage while ΔfbpA mutant would be in a 'late endosome' stage.

The examination of other proteins among the three phagosome samples (**Figure 1** and **Figure 3**), however, indicates that $\Phi_{\Delta fbpA}$ and Φ_{H37Rv} share more similarity than either of them with Φ_{BCG}. In **Figure 1**, it can be seen that, near the data center, more proteins shift slightly toward the Φ_{BCG} vector representing the BCG-infected phagosomes. In **Figure 3**, it can be more clearly seen that there are less proteins differentially expressed in $\Phi_{\Delta fbpA}/\Phi_{H37Rv}$ than in either $\Phi_{BCG}/\Phi_{\Delta fbpA}$ or Φ_{BCG}/Φ_{H37Rv}. The analysis of a limited number of phagosome maturation markers suggests that the BCG- and H37Rv-infected phago-somes share commonality in inhibiting the phagosome maturation. It also suggests that the ΔfbpA-infected phagosomes proceed further in maturation [27]. But the closer proteome composition between the ΔfbpA- and H37Rv-infected phagosomes could be due to the fact that ΔfbpA and H37Rv are very close strains with the difference of a single gene knock-out while BCG is a different species compared to those two. At the meantime, a comparison of the fluorescence microscopy and proteomics results suggests that the modulation of phagosome maturation process does not necessarily need a large change in some key proteins such as those endosome and lysosome markers. A 2-fold change in protein abundance could possibly have induced a change in the phagosome biological process. Proteomic analyses typically use a >2-fold change, preferably a >3-fold change, threshold to discern differentially expressed proteins. Such a threshold does not allow detecting the subtle (≤2-fold) change in some key proteins that may already augment some changes in the biological process of phagocytosis and antigen presentation. The effect of the subtle changes in protein abundance stresses the need to achieve a more sensitive detection of protein abundance change using the proteomics techniques [29]. The improvement in sensitivity to discern

protein differential abundance can be in part achieved with more analysis replicates. While a subtle difference in some key proteins may be sufficient to augment a shift in the phagosome maturation process, a larger difference in some other proteins does not necessarily affect the phagosome maturation process. This is suggested by the larger difference in $\Phi_{BCG}/\Phi_{\Delta fbpA}$ and Φ_{BCG}/Φ_{H37Rv} (**Figure 3**). It would not be surprising that the global phagosomal proteome profile is modulated by different strains of pathogen even though some of those pathogens might share certain common pathogenesis characteristics e.g., inhibition of phagosome maturation.

The proteomic analysis indicates that a larger number of proteins are identified from mitochondria to represent *ca*. 1/3 of the detected proteins. It has been suggested that mitochondria have a similar density with bacteria-containing phagosomes [8]. By using a centrifugation method, the mitochondria might not be separated from the bacteria-containing phagosomes. In addition, auto-phagy of mitochondria might result in some autophagosomes that share similar density with the bacteria-containing phagosomes. In our preliminary studies, the ΔfbpA colocalized into autophagosomes. It also cannot be excluded that some mitochondria could be trapped in the sample phagosomes with the bacteria, although the entrapment of mitochondria and bacteria in the same phagosomes could be a smaller contribution of the mitochondrial proteins to the phagosome sample composition. In fact, mitochondrial proteins have been consistently detected in many phagosome and phagolysome proteomic studies, including the studies of latex-bead containing phagosomes [13] that is presumably purer because the lighter buoyancy of latex-beads allows a more complete separation of the phagosomes from the mitochondria. In a recent study of *Legionella*-containing phagosomes [23], the authors went through a greater length of separation process to purify the phagosomes. The methods employed include elimination of lysosomes with colloidal iron-loading and magnetic separation, elimination of mito-chondria by iodophenylnitrophenyltetrazolium heavy labeling, and degradation of nucleic acid by Benzonase. The percentage of mito-chondrial proteins was reduced to 6.4%. Those results suggest that mitochondria contami-

nation exists during phagosome separation and could be reduced, although not eliminated, with elaborate treatments. The existence of some mitochondrial proteins might not directly affect the protein relative abundance determination if the content of mitochondria is consistent in the phagosome preparations. However, this assumption requires further experiments. On the other hand, a complete elimination of mitochondrial proteins might not be realistic because those proteins could be inherent components of phagosomes given the fact that phagosome biogenesis is a highly dynamic process that recruits variety of intracellular vesicles, cytosolic components, and membrane components. Nevertheless, an elaborate procedure to specifically target mitochondria for removal seems helpful in preparing pure phagosomes [23].

The role of ER in phagocytosis and phagosomal membrane formation is still under debate [8]. While the proteomic analyses of phagosomes in literature have consistently reported ER markers in phagosome preparation, the model of ER-membrane incorporation to the phagosome has been controversial. Two models have been proposed. The conventional phagocytosis model suggests that ER participates in the early phagocytosis process and contributes to a large portion of the phagosomal membrane, probably up to 50% [48]. The opposing phagosome maturation model suggests that phagosome fuses sequentially with early endosomes, late endosomes, and lysosomes. Under this phagosome maturation model, the percentage of ER proteins in the phagosome composition should be relatively small. A major difference between these two models is the fraction of ER proteins in the phagosomal proteome. There has been little doubt that ER proteins are found in phagosome preparations. A quantitative proteomic analysis is needed to resolve the debate over the two opposing models of the role of ER in phagosome formation. We routinely use antibody to calnexin as a marker of ER when we analyzed the phagosome pellets to ensure that they are not contaminated with ER membranes. Our phagosomes are thus relatively free of ER derived contaminants. Our study here supports the model of phagosome maturation in which ER proteins do not represent a large portion of the phagosomal proteins (**Figure 4**). The small number of detected lysosomal

proteins observed in this study also supports that the maturation of the phagosomes containing the three different mycobacterial strains is inhibited or limited [27].

The chaperonin-containing T-complex is part of the phagosome network [6] and is enriched in the *cellular_component* GO hierarchy (**Figure 4**). Three of the six proteins detected in this complex were upregulated in the ΔfbpA-infected phagosomes versus those infected by either BCG or H37Rv (**Figure 3**). This T-complex may participate in the phagosome maturation to process engulfed pathogens. Cytoskeleton proteins and ribosome proteins are also consistently detected in other phagosome studies [6, 13, 23]. Compared to the *Legionella*-containing phagosomes that were purified with selective removal of mitochondria and lysosomes [23], the percentage of cytoskeleton proteins or ribosomal proteins detected in our study is similar. The 12 detected chromatin proteins could be due to nuclei contamination but we cannot rule out that they are part of the phagosome constituents because these organelles are closely connected to the nucleus and the ER and cytoskeleton proteins are consistently detected as phagosomal proteins in many studies of phagosomes.

We compare the 321 phagosomal proteins identified in this study with the 2415 phagosomal proteins identified by Trost et al from the latex-bead-containing phagosomes in INF-γ activated and non-stimulated mouse macrophages [13]. The 2415 proteins detected by Trost et al include 250 but not all of the 321 proteins identified in our study. Because the number of phagosomal proteins identified by Trost et al is about seven times of that in this study, many of the 71 proteins detected in this work but not in the work by Trost et al [13] are likely unique to the mycobacterial infections. Some of these 71 proteins could also be due to the difference in cell lines employed in the two studies.

This study opens up a new avenue to further study the modulation of phagosomes by mycobacterial infection. Among the markers selectively enriched on mycobacterial phagosomes we found interesting observations. The marker Cdc42 was enriched on wild type H37Rv-, unlike BCG- or ΔfbpA mutant-containing phagosomes. Cdc42 is enriched by 7 and 57 folds on H37Rv phagosomes

compared to ΔfbpA and BCG phagosomes respectively. The *M. avium* fadD2 gene binds to Cdc42 to enter epithelial cells and we speculate Mtb does the same since its invasion of epithelial cells is well known [49]. It is established that Rab11b facilitates the ability to recycle membrane components during giant cell formation where macrophages fuse with each other [50]. Using immunofluorescence, we found that Rab11b is enriched on H37RV wild type phagosomes in human macrophages and only H37Rv had the phenotype to induce multinucleate giant cells through fusion of macrophages (Estrella et al, communicated to Cellular Microbiology, 2009). In this study, we found that Rab11b is enriched by about 20 and 40 times on H37Rv phagosomes compared to ΔfbpA and BCG respectively, consistent with the immunofluorescence result.

We also found that Nicastrin was enriched by about 6 and 60 times on H37Rv phagosomes compared to ΔfbpA and BCG respectively. The enrichment of Nicastrin on wild type H37Rv opens up a new avenue of research. Together with presenilin, and Aph1, it forms the gamma secretase enzyme complex that is an integral part of phagosomes. It is thought to mediate protein cleavage within phagosome and thus facilitate peptide antigen presentation [51]. We found Nicastrin also on the phagosomes infected by the three mycobacterial strains. The roles of Nicastrin and other important markers need to be investigated further within a broader context of the modulation of the recruitment of other proteins, which will be afforded by a systems approach as shown in this pilot study.

Conclusion

We have investigated the BMA.A3 phagosomal proteome modulated by three different mycobacterial strains including the ΔfbpA, BCG, and H37Rv. Of the two opposing conventional models of the role of ER in phagosome formation, our results support the model of phagosome maturation in which ER proteins do not represent a large portion of the phagosomal proteins. In this phagosome maturation model, the phagosome fuses sequentially with early endosomes, late endosomes, and lysosomes. With the GO hierarchy analysis of the mouse proteins, we found that the number of lysosomal proteins represent <3% of the identified proteins. This result is consistent with the fact that H37Rv and BCG inhibit the phagosome maturation and the ΔfbpA limits the phagosome maturation. Within the sensitivity limit of the proteomic approach to discern protein abundance changes, several key endosome and lysosome markers are not found to be differentially expressed among the phagosomes infected with the three different mycobacterial strains. Meanwhile, there are other proteins that are regulated at larger amplitude. These results suggest that the different mycobacterial strains apparently modulate the phagosomal proteome even though they share some common pathogenic characteristics e.g., inhibition of phagosome maturation. The results also suggest that the phagosome maturation could be modulated by a small change in some key proteins while a large change in some other protein need not affect the phagosome maturation process. The proteomics and system biology approaches adapted in this study demonstrate the advantage of a global analysis of the phagosomal proteome. With the network analysis at the systems level and more in-depth and precise proteomic study, we anticipate that new insights will be brought forward into the modulation of the phagosomal proteome by different antigenic or pathogenic strains of mycobacteria.

Acknowledgements

Address correspondence to: Qingbo Li, PhD, [3]Department of Microbiology and Immunology, University of Illinois at Chicago, Chicago, IL 60612, USA, Tel: 312-413-9301; Fax: 312-413-9303. E-Mail: qkli@uic.edu

References

[1] Sturgill-Koszycki S, Schlesinger PH, Chakraborty P, Haddix PL, Collins HL, Fok AK, Allen RD, Gluck SL, Heuser J and Russell DG. Lack of acidification in Mycobacterium phagosomes produced by exclusion of the vesicular proton-ATPase. Science 1994; 263: 678-681.

[2] Philips JA. Mycobacterial manipulation of

vacuolar sorting. Cell Microbiol 2008; 10: 2408-2415.

[3] Stuart LM and Ezekowitz RA. Phagocytosis: elegant complexity. Immunity 2005; 22: 539-550.

[4] Gotthardt D, Warnatz HJ, Henschel O, Bruckert F, Schleicher M and Soldati T. High-resolution dissection of phagosome maturation reveals distinct membrane trafficking phases. Mol Biol Cell 2002; 13: 3508-3520.

[5] Underhill DM and Ozinsky A. Phagocytosis of microbes: complexity in action. Annu Rev Immunol 2002; 20: 825-852.

[6] Stuart LM, Boulais J, Charriere GM, Hennessy EJ, Brunet S, Jutras I, Goyette G, Rondeau C, Letarte S, Huang H, Ye P, Morales F, Kocks C, Bader JS, Desjardins M and Ezekowitz RA. A systems biology analysis of the Drosophila phagosome. Nature 2007; 445: 95-101.

[7] Desjardins M and Griffiths G. Phagocytosis: latex leads the way. Curr Opin Cell Biol 2003; 15: 498-503.

[8] Rogers LD and Foster LJ. The dynamic phagosomal proteome and the contribution of the endoplasmic reticulum. Proc Natl Acad Sci U S A 2007; 104: 18520-18525.

[9] Shui W, Sheu L, Liu J, Smart B, Petzold CJ, Hsieh TY, Pitcher A, Keasling JD and Bertozzi CR. Membrane proteomics of phagosomes suggests a connection to autophagy. Proc Natl Acad Sci U S A 2008; 105: 16952-16957.

[10] Jutras I, Houde M, Currier N, Boulais J, Duclos S, LaBoissiere S, Bonneil E, Kearney P, Thibault P, Paramithiotis E, Hugo P and Desjardins M. Modulation of the phagosome proteome by interferon-gamma. Mol Cell Proteomics 2008; 7: 697-715.

[11] Robinson N, Kolter T, Wolke M, Rybniker J, Hartmann P and Plum G. Mycobacterial phenolic glycolipid inhibits phagosome maturation and subverts the pro-inflammatory cytokine response. Traffic 2008; 9: 1936-1947.

[12] Garin J, Diez R, Kieffer S, Dermine JF, Duclos S, Gagnon E, Sadoul R, Rondeau C and Desjardins M. The phagosome proteome: insight into phagosome functions. J Cell Biol 2001; 152: 165-180.

[13] Trost M, English L, Lemieux S, Courcelles M, Desjardins M and Thibault P. The phagosomal proteome in interferon-gamma-activated macrophages. Immunity 2009; 30: 143-154.

[14] Gotthardt D, Blancheteau V, Bosserhoff A, Ruppert T, Delorenzi M and Soldati T. Proteomics fingerprinting of phagosome maturation and evidence for the role of a Galpha during uptake. Mol Cell Proteomics 2006; 5: 2228-2243.

[15] Marion S, Laurent C and Guillen N. Signalization and cytoskeleton activity through myosin IB during the early steps of phagocytosis in Entamoeba histolytica: a proteomic approach. Cell Microbiol 2005; 7: 1504-1518.

[16] Kovarova H, Halada P, Man P, Golovliov I, Krocova Z, Spacek J, Porkertova S and Necasova R. Proteome study of Francisella tularensis live vaccine strain-containing phagosome in Bcg/Nramp1 congenic macrophages: resistant allele contributes to permissive environment and susceptibility to infection. Proteomics 2002; 2: 85-93.

[17] Sturgill-Koszycki S, Haddix PL and Russell DG. The interaction between Mycobacterium and the macrophage analyzed by two-dimensional polyacrylamide gel electrophoresis. Electrophoresis 1997; 18: 2558-2565.

[18] Mills SD and Finlay BB. Isolation and characterization of Salmonella typhimurium and Yersinia pseudotuberculosis-containing phagosomes from infected mouse macrophages: Y. pseudotuberculosis traffics to terminal lysosomes where they are degraded. Eur J Cell Biol 1998; 77: 35-47.

[19] Luhrmann A and Haas A. A method to purify bacteria-containing phagosomes from infected macrophages. Methods Cell Sci 2000; 22: 329-341.

[20] Fernandez-Mora E, Polidori M, Luhrmann A, Schaible UE and Haas A. Maturation of Rhodococcus equi-containing vacuoles is arrested after completion of the early endosome stage. Traffic 2005; 6: 635-653.

[21] Kima PE and Dunn W. Exploiting calnexin expression on phagosomes to isolate Leishmania parasitophorous vacuoles. Microb Pathog 2005; 38: 139-145.

[22] Urwyler S, Nyfeler Y, Ragaz C, Lee H, Mueller LN, Aebersold R and Hilbi H. Proteome analysis of Legionella vacuoles purified by magnetic immunoseparation reveals secretory and endosomal GTPases. Traffic 2009; 10: 76-87.

[23] Shevchuk O, Batzilla C, Hagele S, Kusch H, Engelmann S, Hecker M, Haas A, Heuner K, Glockner G and Steinert M. Proteomic analysis of Legionella-containing phagosomes isolated from Dictyostelium. Int J Med Microbiol 2009;

[24] Fratti RA, Vergne I, Chua J, Skidmore J and Deretic V. Regulators of membrane trafficking and Mycobacterium tuberculosis phagosome maturation block. Electrophoresis 2000; 21: 3378-3385.

[25] Rupper A and Cardelli J. Large-scale purification of latex bead phagosomes from mouse macrophage cell lines and subsequent preparation for high-throughput quantitative proteomics. Methods Mol Biol 2008; 445: 339-351.

[26] Copenhaver RH, Sepulveda E, Armitige LY, Actor JK, Wanger A, Norris SJ, Hunter RL and Jagannath C. A mutant of Mycobacterium tuberculosis H37Rv that lacks expression of antigen 85A is attenuated in mice but retains vaccinogenic potential. Infect Immun 2004; 72: 7084-7095.

[27] Katti MK, Dai G, Armitige LY, Rivera Marrero C,

Daniel S, Singh CR, Lindsey DR, Dhandayuthapani S, Hunter RL and Jagannath C. The Delta fbpA mutant derived from Mycobacterium tuberculosis H37Rv has an enhanced susceptibility to intracellular antimicrobial oxidative mechanisms, undergoes limited phagosome maturation and activates macrophages and dendritic cells. Cell Microbiol 2008; 10: 1286-1303.

[28] Rao PK, Rodriguez GM, Smith I and Li Q. Protein dynamics in iron-starved Mycobacterium tuberculosis revealed by turnover and abundance measurement using hybrid-linear ion trap-fourier transform mass spectrometry. Anal Chem 2008; 80: 6860-6869.

[29] Li Q and Roxas BA. An assessment of false discovery rates and statistical significance in label-free quantitative proteomics with combined filters. BMC Bioinformatics 2009; 10: 43.

[30] Rao P and Li Q. Principal Component Analysis of Proteome Dynamics in Iron-Starved Mycobacterium Tuberculosis. Journal of Proteomics and Bioinformatics 2009; 2: 19-31.

[31] Choi H, Ghosh D and Nesvizhskii AI. Statistical validation of peptide identifications in large-scale proteomics using the target-decoy database search strategy and flexible mixture modeling. J Proteome Res 2008; 7: 286-292.

[32] http://tools.proteomecenter.org/wiki/index.php?title=Software:TPP.

[33] Rao PK, Roxas BA and Li Q. Determination of global protein turnover in stressed mycobacterium cells using hybrid-linear ion trap-fourier transform mass spectrometry. Anal Chem 2008; 80: 396-406.

[34] Andreev VP, Li L, Cao L, Gu Y, Rejtar T, Wu SL and Karger BL. A new algorithm using cross-assignment for label-free quantitation with LC-LTQ-FT MS. J Proteome Res 2007; 6: 2186-2194.

[35] Finney GL, Blackler AR, Hoopmann MR, Canterbury JD, Wu CC and MacCoss MJ. Label-free comparative analysis of proteomics mixtures using chromatographic alignment of high-resolution muLC-MS data. Anal Chem 2008; 80: 961-971.

[36] Apraiz I, Mi J and Cristobal S. Identification of proteomic signatures of exposure to marine pollutants in mussels (Mytilus edulis). Mol Cell Proteomics 2006; 5: 1274-1285.

[37] Ivosev G, Burton L and Bonner R. Dimensionality reduction and visualization in principal component analysis. Anal Chem 2008; 80: 4933-4944.

[38] Ashburner M, Ball CA, Blake JA, Botstein D, Butler H, Cherry JM, Davis AP, Dolinski K, Dwight SS, Eppig JT, Harris MA, Hill DP, Issel-Tarver L, Kasarskis A, Lewis S, Matese JC, Richardson JE, Ringwald M, Rubin GM and Sherlock G. Gene ontology: tool for the unification of biology. The Gene Ontology Consortium. Nat Genet 2000; 25: 25-29.

[39] Shannon P, Markiel A, Ozier O, Baliga NS, Wang JT, Ramage D, Amin N, Schwikowski B and Ideker T. Cytoscape: a software environment for integrated models of biomolecular interaction networks. Genome Res 2003; 13: 2498-2504.

[40] von Mering C, Jensen LJ, Kuhn M, Chaffron S, Doerks T, Kruger B, Snel B and Bork P. STRING 7--recent developments in the integration and prediction of protein interactions. Nucleic Acids Res 2007; 35: D358-362.

[41] http://string.embl.de/.

[42] http://www.genome.jp/kegg/.

[43] Mollenkopf HJ, Jungblut PR, Raupach B, Mattow J, Lamer S, Zimny-Arndt U, Schaible UE and Kaufmann SH. A dynamic two-dimensional polyacrylamide gel electrophoresis database: the mycobacterial proteome via Internet. Electrophoresis 1999; 20: 2172-2180.

[44] Rosenkrands I, King A, Weldingh K, Moniatte M, Moertz E and Andersen P. Towards the proteome of Mycobacterium tuberculosis. Electrophoresis 2000; 21: 3740-3756.

[45] Monahan IM, Betts J, Banerjee DK and Butcher PD. Differential expression of mycobacterial proteins following phagocytosis by macrophages. Microbiology 2001; 147: 459-471.

[46] Wong DK, Lee BY, Horwitz MA and Gibson BW. Identification of fur, aconitase, and other proteins expressed by Mycobacterium tuberculosis under conditions of low and high concentrations of iron by combined two-dimensional gel electrophoresis and mass spectrometry. Infect Immun 1999; 67: 327-336.

[47] Sassetti CM, Boyd DH and Rubin EJ. Genes required for mycobacterial growth defined by high density mutagenesis. Mol Microbiol 2003; 48: 77-84.

[48] Gagnon E, Duclos S, Rondeau C, Chevet E, Cameron PH, Steele-Mortimer O, Paiement J, Bergeron JJ and Desjardins M. Endoplasmic reticulum-mediated phagocytosis is a mechanism of entry into macrophages. Cell 2002; 110: 119-131.

[49] Harriff MJ, Danelishvili L, Wu M, Wilder C, McNamara M, Kent ML and Bermudez LE. Mycobacterium avium genes MAV_5138 and MAV_3679 are transcriptional regulators that play a role in invasion of epithelial cells, in part by their regulation of CipA, a putative surface protein interacting with host cell signaling pathways. J Bacteriol 2009; 191: 1132-1142.

[50] Zhao H, Ettala O and Vaananen HK. Intracellular membrane trafficking pathways in bone-resorbing osteoclasts revealed by cloning and subcellular localization studies of small GTP-binding rab proteins. Biochem Biophys Res Commun 2002; 293: 1060-1065.

[51] Jutras I, Laplante A, Boulais J, Brunet S,

Thinakaran G and Desjardins M. Gamma-secretase is a functional component of phagosomes. J Biol Chem 2005; 280: 36310-36317.